

Ground surface deformation monitoring all over Japan by InSAR using ALOS-2 data (first report)

MORISHITA, Yu^{1*} ; YAMADA, Shinya¹

¹GSI of Japan

The Geospatial Information Authority of Japan (GSI) monitored ground surface deformation in 66 areas of volcano, subsidence and landslide all over Japan by InSAR using ALOS SAR data from 2006 to 2011. After ALOS stopped its operation in May 2011, the regular InSAR analysis could not be continued.

ALOS-2, a successor of ALOS, was launched on 24 May, 2014 and started the basic observation on 4 August. The observed SAR data has been provided since 25 November, 2014. GSI restarts the monitoring by InSAR using ALOS-2 data. The target area is all land areas all over Japan, expanded from the particular areas in the era of ALOS. Basically all data acquired by the basic observation mode will be processed. These advancements of the monitoring strategy from the time of ALOS are achieved by the constantly short baseline of ALOS-2 and the improvement of our processing system.

InSAR results will be published as one of the layers of the geospatial information library on GSI Maps, a web map provided by GSI and where various geospatial information can be shown as well as background maps. This style of publication would make it easy to interpret the InSAR results and identify the location of the deformation, and promote the use of InSAR results. The interpretation of the InSAR results will be added in the future.

In ALOS-2 Basic Observation Scenario, disaster base map observations by various observation modes and off-nadir angles are planned for one year after the start of the basic observation. Therefore the amount of the available data for InSAR analysis is not large because the InSAR analysis requires two or more data acquired by the same mode and off-nadir angle. The full operation of the monitoring will start around August 2015.

In this presentation we report the first InSAR results using a limited amount of ScanSAR data and the future plan of the monitoring.

Keywords: InSAR, ALOS-2, deformation, subsidence, landslide, volcano

Crustal deformation derived from the northern Nagano prefecture earthquake detected by InSAR analysis using ALOS-2 data

YARAI, Hiroshi^{1*} ; KOBAYASHI, Tomokazu¹ ; MORISHITA, Yu¹ ; YAMADA, Shinya¹ ; TOBITA, Mikio¹

¹GSI of Japan

ALOS-2, launched by JAXA on 24 May, 2014, is the newest L-band SAR satellite. Applying interferometric SAR (InSAR) analysis using ALOS-2 data to the northern Nagano prefecture earthquake (Mj 6.7, occurred on 22 November, 2014), we succeeded in a mapping a coseismic ground displacement. We used ALOS-2/PALSAR-2 data acquired by both right and left look direction from descending orbits. The interferograms suggest that fault motion of the earthquake has reverse dip slip with left-lateral motion on an east dipping plane. The most concentrated crustal deformation is located in the southern part of rupture area near epicenter of the mainshock, showing displacements toward to the satellite with ~1 m at the maximum. Clear displacement discontinuity is recognized along western margin of the large crustal deformation area, which is just on the Kamishiro fault. We invert the InSAR results with GNSS data to construct slip distribution model of the earthquake. From fringe pattern of InSAR images, we assumed that a fault plane changes dip angle at 2 km depth, low dip angle shallower than 2 km and steep dip angle deeper than 2 km. Our preliminary model shows large (over 1 m) slip on southern part of shallower segment and moderate (~1 m) slip around hypocenter of the mainshock on deeper segment. Both segments demonstrate reverse dip slip with left-lateral motion. On the other hand, no significant slip is estimated on northern part of shallower segment.

Keywords: Northern Nagano Prefecture earthquake, ALOS-2, InSAR

ALOS2-PALSAR2 Interferometry on snow covered mountaneous area in Hokkaido: Tokachidake Volcano and Vicinity

MURAKAMI, Makoto^{1*}

¹Institute of Seismology and Volcanology, Hokkaido Univ.

A repeat pass interferometry using spaceborne L-band synthetic-aperture radar provides a good coherency even on a vegetated area. It has already become an indispensable geodetic tool to detect spatial distribution of crustal deformation. However, if the earth surface is covered by snow at a cold district covered, we suffer from loss of coherence mainly caused by the change of reflection conditions due to a snowpack.

A relatively large dielectric constant of dry snow brings changes of the microwave propagation velocity and traveling distance. Nevertheless, details of a phase change by snowpack were left untouched, because the basic coherence was considered to be lost when the earth surface is covered by snow or ice.

ALOS2 satellite was launched by Japanese space agency, JAXA in May, 2014. This is a satellite dedicated solely for SAR mission. It is equipped with PALSAR2 which is the next generation L band sensor. Various improvements have been implemented in this satellite. As a result it is expected to provide high coherency for repeat pass InSAR for different areas on the globe. If an observation for snow covered target is also becomes possible, it is a significant step forward for facilitation of a geodetic monitoring in winter over a volcano season where the terrestrial access is very limited.

To validate such possibility several InSAR analyses were carried out using PALSAR2 data acquired on August 14, December 4, the 18, 2014, and January 15, 2015. The target area includes Tokachidake and Taisetsu volcanic chains.

Relatively good coherence was obtained for the pair spanning December 4 and 18 despite a heavy snow fall experienced one day before the second acquisition. This indicates a possibility that a good coherence is achievable for a snow covered target, if the other conditions are favorable. It is noteworthy that the coherence was also maintained around volcano summit where the ground is mostly composed with lava and breccia and almost no vegetation is found. This is an encouraging finding for the achievement of geodetic monitoring around vents and craters of volcanoes located in cold region with similar setting. On the other hand, some interesting phase patterns having correlation with land characteristics (forest, cultivated field, and city, etc.) are found on flat regions. Those might suggest that the phase change caused by snowpack depends on bouncing mechanisms of microwave. In the presentation, more details of those findings will be covered.

The PALSAR2 data used here were acquired and provided by JAXA through the Working Group for special study on application of satellite remote sensing technology for volcanic monitoring, organized under the umbrella of the Coordinating Committee for Prediction of Volcanic Eruption.

Keywords: crustal deformation, InSAR, remote sensing, satellite, volcano, snowpack

Interferometry of PALSAR-2 images for crustal deformation study

HASHIMOTO, Manabu^{1*}

¹Disaster Prevention Research Institute, Kyoto University

Since the first acquisition of image in June, 2014, PALSAR-2 has been operated satisfactorily. Since the beginning of operation, earthquake and volcanic activities occurred and crustal deformations associated with these events were detected. In this paper, we examine coherence, accuracy of PALSAR-2 interferograms and observed deformations for the Ontake eruption, Northern Nagano (Mjma6.7) and Southern Tokushima (Mjma5.1) earthquakes.

For the analysis we used the RINC (developed by Dr. Ozawa, NIED) and Gamma software, and the digital ellipsoidal models or ASTER-GDEM ver.2 for coregistraion and reduction of topography phase. UBS mode images with 3-m azimuthal resolution were analyzed.

We used two pairs of PALSAR-2 images acquired on August 22 and October 3, and August 18 and October 13. Both pairs were acquired on ascending orbits with right-looking configuration. Incidence angles and perpendicular baselines are 36 deg. and 5 m, and 53 deg. and 24 m, respectively. We recognized high coherence in both interferograms despite of mountainous region. However we also recognized systematic deviation from the synthetic LOS displacements at GEONET stations in the scene and its standard deviations were estimated 4~5 cm. LOS decrease was observed near the summit of Ontake volcano, but no significant deformation was found in the surrounding region. Therefore we can conclude that the deformation was localized in the vicinity of the summit.

We analyzed two pairs of images acquired on October 2 and November 27, and September 19 and November 28. The former pair is observed from a descending orbit with left-looking configuration, while the latter is from an ascending orbit with right-looking. Incidence angle and perpendicular baseline are 36 deg. and 6 m, 40 deg. and 112 m, respectively. We recognized high coherence but lines of low coherence on the hanging wall side of source fault. These belts might coincide with surface ruptures of subsidiary faults such as backstop. We estimated slip distribution from interferograms and obtained up to 1.3 m thrust on an ESE dipping plane in a depth range shallower than 5 km.

We also analyzed two pairs of PALSAR-2 images acquired before and after the Southern Tokushima earthquake, but did not observed any significant surface displacements.

Keywords: PALSAR-2, crustal deformation, SAR interferometry

Surface deformation in the Shinmoe-dake crater detected by Pi-SAR-L2/InSAR

OZAWA, Taku^{1*} ; MIYAGI, Yosuke¹ ; SHIMADA, Masanobu²

¹National Research Institute for Earth Science and Disaster Prevention, ²Japan Aerospace Exploration Agency

Shinmoe-dake in the Kirishima volcano group erupted in January 2011. Ozawa and Kozono (2013) analyzed spaceborne SAR images and revealed that lava extruded to the crater with constant rate of $88.7\text{m}^3/\text{sec}$ during January 29 and 31; it was after three sub-Plinian eruptions. After that, eruption type changed to Vulcanian eruptions, and frequency of eruption occurrence decreased with time. Since last eruption of September 2011, eruption has not occurred. However, Miyagi et al. (2014) carried out InSAR analysis with RADARSAT-2 and TerraSAR-X and revealed that lava extrusion had continued. Although lava extrusion rate tended to decrease with time, extrusion rate of $50\text{-}100\text{m}^3/\text{day}$ was estimated in May 2013.

In this study, we attempt to apply InSAR analysis with JAXA's airborne SAR data (sensor name: Pi-SAR-L2). SAR data used in this study were observed on 13 Sep. 2013 and 7 Aug. 2014 from three flight paths. In the simulation of topographic fringes, we used digital terrain model which was generated by SBAS analysis with RADARSAT-2 acquired after the last eruption. Large non-deformation component remained in differential SAR interferogram. Then we confined analysis area to $1\text{km} \times 1\text{km}$ around the crater and removed its component so that phase difference outside of the crater became negligible, assuming its component to be a plane. Obtained results show slant-range shortening in the crater, and its area is almost the same with results from spaceborne InSAR. Since slant-range changes from three flight paths were obtained, we estimated three-dimensional displacement map from them. Uplift exceeding 20cm was found. On the other hand, horizontal displacement with radial direction was found surrounding uplift area, but its amount was less than 3cm in most area. It suggests that viscosity of extruded lava is high and that fluidity to horizontal direction was low.

The lava extrusion volume during 13 Sep. 2013 and 7 Aug. 2014 was estimated to 10044m^3 from obtained uplift map. On the other hand, spaceborne SAR images up to 14 Apr. 2014 were available, and the lava extrusion volume during 13 Sep. 2013 and 16 Apr. 2014 was estimated to $7507\text{-}7704\text{m}^3$ from InSAR analysis using them. Then the lava extrusion volume during 16 Apr. 2014 and 13 Sep. 2013 was estimated to $2340\text{-}2537\text{m}^3$. Huppert and Woods (2002) indicated the model for temporal change of lava extrusion in the case that shallow magma chamber with overpressure exists. We fitted extrusion rates from spaceborne InSAR analysis to the model in the case that magma is injected to shallow magma chamber from deep source, and the lava extrusion volume of 2339m^3 during 16 Apr. 2014 and 13 Sep. 2013 was estimated, corresponding to that from observed one. Miyagi et al. (2014) suggested continuous magma supply to shallow magma chamber from spaceborne InSAR analysis by May 2013, and result in this study suggests that such magma supply decreased.

Acknowledgements. Pi-SAR-L2 data was provided based on cooperative research with JAXA. TerraSAR-X and/or TanDEM-X data were provided on the cooperative activities between German Aerospace Center (DLR) and JAXA in the field of Satellite Disaster Monitoring.

Keywords: airborne SAR, InSAR, Shinmoe-dake, crater, lava, deformation

Evaluation of noise equivalent σ_0 for Pi-SAR-L2 and PALSAR-2.

WATANABE, Manabu^{1*}; MOTOHKA, Takeshi¹; OHKI, Masato¹; NATSUAKI, Ryo¹; YONEZAWA, Chinatsu²; SHIMADA, Masanobu¹

¹JAXA, ²Tohoku University

The noise equivalent σ_0 (NESZ) were evaluated to the data simultaneously observed with Pi-SAR-L2 and PALSAR-2 by full polarimetry mode. The observation were done on Sept. 11, 2014 over Sendai airport. Fast Fourier transforms (FFTs) was applied to the data, and 10, 20, 30, 40, 50 dB random noise were added in the frequency domain. Inverse FFTs was applied to obtain the time domain data. The change of σ_0 for the runway in the Sendai airport was examined, and the NESZ for Pi-SAR-L2 and PALSAR-2 were evaluated from the data. Estimated NESZ were -46.2, -60.5, -61.0, -55.0 dB for σ_0 HH, HV, VH, VV of Pi-SAR-L2 data, and -40.3, -50.0, -51.3, -43.0 dB of PALSAR-2 data. The NESZ for the Pi-SAR-L2 was 6 to 12 dB better than those for the PALSAR-2.

The Pi-SAR-L2 σ_0 profile for the area, where the incident angle is same, were compared with the PALSAR-2 σ_0 for each polarization. The area, where σ_0 is more than -20 dB shows almost same profile, and shows same σ_0 . On the other hand, the area, where σ_0 is less than -20 dB shows the difference. The difference was not explained by the NESZ estimated above. One of the possible causes for the higher NESZ may be higher azimuth ambiguity for the PALSAR-2 data.

Keywords: Full polarimetry,, SAR

Detection of meso- and submeso-scale ocean fronts using Synthetic Aperture Radar (SAR) and Optical data

ISOGUCHI, Osamu^{1*}

¹Remote Sensing Technology Center (RESTEC)

Synthetic aperture radar (SAR) can image ocean surface roughness with high spatial resolution (~10m) and operationally detect information on wind speed and wave, which are related to ocean surface roughness. One of main factors by which surface roughness is modulated is convergence and divergence of surface currents and it has been reported that a large current shear is imaged as line-shaped high NRCS on a SAR image. With a combination of c-band SAR and optical images, a study on upper ocean dynamics has been reported. In the present study, information of ocean fronts with meso- and submeso-scales are detected using L-band SAR (PALSAR-2) and MODIS SST/Chl-a images. The MODIS data we used, which are processed and provided in near-real-time by JAXA/EORC, are observed in the Northwestern Pacific at October 25, 2014 01:11(UT), while PALSAR-2 data that are provided by JAXA within the framework of the 4th ALOS Research Announcement are acquired at October 25, 2014 14:17(UT), about 13 hours time gap for the MODIS acquisition.

In order to make fine structure visible, an about 20-km high-pass filtering is applied for the PALSAR-2 NRCS image after eliminating incidence angle-dependent average signals. This PALSAR-2 contrast image is then compared with the MODIS SST and Chl-a images. The comparison shows that the positions of line-shaped bright and dark patterns in the contrast images correspond with large SST gradients, i.e., SST fronts. This feature is consistent with a general theory that divergence and convergence areas induced by large current shear are imaged dark and bright, respectively, through the modulation of ocean surface roughness. Moreover, the comparison with the Chl-a image represents some local Chl-a maximum along the line-shaped patterns in the PALSAR-2 contrast image. It is suggested that the local increase of Chl-a is induced by upwelling caused by submeso-scale front phenomena. The PALSAR-2 contrast image is thus expected to give useful information on the upper ocean dynamics. In addition to that, since the detected line-shaped patterns might represent "Shiome" and are related to Chl-a concentration, it is interesting to investigate their relationship with fishing grounds.

Keywords: PALSAR-2, ocean front, submesoscale

ALOS-2 / PALSAR-2 ScanSAR-ScanSAR interferometry observation for Philippine Mayon Volcano analysis

NATSUAKI, Ryo^{1*} ; MOTOHKA, Takeshi¹ ; WATANABE, Manabu¹ ; OHKI, Masato¹ ; SHIMADA, Masanobu¹

¹Earth Observation Research Center, Japan Aerospace Exploration Agency

On September 14 - 18, 2014, Mayon Volcano recorded some activities including lava flows. Before and the after those activities, Advanced Land Observation Satellite-2 (ALOS-2) observed the volcano on September 4 (Scene ID: ALOS2015233350-140904) and October 16 (Scene ID: ALOS2021443350-141016). ALOS-2 carries the state-of-the-art L-band Synthetic Aperture Radar (SAR), the Phased Array type L-band Synthetic Aperture Radar-2 (PALSAR-2) [1]. It has 3m spatial resolution with 50km swath in ultra-fine mode. However, in those observations, 100m x 100m resolution with 350km swath ScanSAR mode was scheduled. No better resolution image was taken during the activities by ALOS-2.

In this paper, we tried interferometric SAR (InSAR) analysis for Mayon volcano with those pair of two ScanSAR images. There are two requirements for the ScanSAR ? ScanSAR interferometry. One is the time synchronization between two observation and the other is the accurate co-registration. PALSAR-2 is designed to have 90% or more burst synchronization. However, as PALSAR-2 was under calibration those days, some pairs have less synchronization ratio. Fortunately, the pair we used marked approximately 53.6% of burst synchronization which is enough high for the interferometry. For the co-registration, in this paper, we applied a local co-registration method using phase gradient estimation from amplitude information proposed in [2], in addition to the popular cross-correlation and geometrical co-registration.

We found some low coherency parts at the summit and the southwest skirt of the mountain. Those low coherency areas represent the surface change caused by the lava or rock fall. On the other hand, no significant deformation was found in the interferogram. These results indicates that this activity was not large enough to make a detectable deformation for 100m resolution SAR interferometry.

References

[1] Kankaku Y. et.al. , "PALSAR-2 Launch and Early Orbit Status" IEEE Geoscience and Remote Sensing Symposium 2014, pp. 3410 - 3412.

[2] R. Natsuaki and A. Hirose, "Performance improvement of InSAR local co-registration with multiresolution interferogram," Asia-Pacific Conference on Synthetic Aperture Radar (APSAR) 2013 Tsukuba, Proc, WE2.R3.1, Tsukuba Japan, September 2013.

Keywords: ALOS-2, PALSAR-2, ScanSAR-ScanSAR interferometry, Interferometric Synthetic Aperture Radar

On the phase linking of distributed scatterers - improvement of measurement density in non-urban areas-

KOBAYASHI, Tomokazu^{1*} ; SAMIEI-ESFAHANY, Sami² ; HANSSEN, Ramon F.²

¹GSI of Japan, ²Delft University of Technology

Preface: Persistent scatterer interferometry (PSI) makes use of points with temporally coherent phase to achieve high accuracy measurements. However, in non-urban environments, the PS density is generally very low and distributed scatterers (DS) are dominant. Thus, it is difficult to monitor crustal deformation in a mountainous area where many active faults/volcanoes are located. To improve the spatial density of the measurement points, the use of DS, in which the phase quality should be comparable to PS, is indispensable.

Phase Linking: The small baselines subsets (SBAS) approach has been developed to extract high-quality phase information from DS. The SBAS, however, requires reliable phase unwrapping of each single interferogram. On the other hand, different approaches have been recently proposed (e.g., Monti-Guarnieri et al, 2008), in which the retrieval of phase time series is done "before" unwrapping. In this method, the single-master phase time series is optimized on the basis of coherence information using all the multilooked "wrapped" interferograms. The optimal phases are obtained as the maximum likelihood estimate of a complex circular Gaussian distribution for multilooked (statistically homogeneous) pixels. This approach is called phase linking as the phases stem from the results of linking all the interferogram phases.

Feasibility test by simulated data: To confirm the effectiveness and to test how well our algorithm works, we first applied it to simulated data. We generated a data set of 24 SLC images with 50 by 50 pixels, in which deformation with a constant speed is included and two kinds of (temporally-decreasing and seasonally changing) coherence matrices were used to simulate the decorrelation noise. A small fringe pattern can be recognized from standard master-slave interferograms with multilooking of 5 by 5, while the estimates by the phase linking could reproduce the true deformation for all interferograms. The standard deviation of the residual from the true phases is close to the theoretical lower limit, namely, Cramér-Rao bound, with a difference of about 0.1-0.2 rad at maximum for all interferometric pairs. On the other hand, there are large differences of about 1.5 rad at maximum for simple multilooked interferograms.

Application to actual data: We applied the method to ALOS/PALSAR data observing Japanese mountainous area, in and around Midagahara volcano where grass/trees cover the land. Only 12 SAR images are available due to the long-term snow-covered-land. We compared the results of a standard PSI analysis. In PSI analysis, the amplitude dispersion method to pick up PS candidates does not have a good performance for small data set, thus we used also the signal-to-clutter ratio method. For DS analysis, we first picked up statistically homogeneous pixels for multilooking by applying the 2-sample KS-test (Ferretti et al., 2011), and then conducted the phase linking. To get the same quality points for both analyses, we used the spatio-temporal consistency as a quality indicator (Hanssen et al., 2008) to select final measurement points. Resultantly, the PSs of 7094 pixels were obtained in full pixel size of 720000, while we could get the optimized DSs of 82138, leading that the observation density significantly improves. In this analysis, we found locally-distributed inflational ground deformation in the geothermal area. The increase of measurement point density contributes to grasp the spatial extent of inflational ground deformation. We can identify that the phase linking of DSs effectively works well for crustal deformation observation in mountainous area.

Acknowledgment: The SAR data obtained using the ALOS/PALSAR were provided by the Japan Aerospace Exploration Agency (JAXA). The ownership of PALSAR data belongs to METI (Ministry of Economy, Trade and Industry) and JAXA.

Keywords: Phase linking, Distributed scatterers, InSAR time series analysis, Persistent scatterer interferometry (PSI)

Condition for water infiltration in snowy highland marshes based on ALOS/PALSAR data analysis

TOYOSAKI, Norihisa¹ ; OGAWA, Yoshiko^{1*} ; HISADA, Yasuhiro¹ ; DEMURA, Hirohide¹ ; SOBUE, Shinichi²

¹Univ. of Aizu, ²RESTEC

We have been studying how to monitor the hydrological environment of snowy highland marshes by using remote sensing. The data from L-band radar PALSAR (The Phased Array type L-band Synthetic Aperture Radar) onboard ALOS (Advanced Land Observing Satellite "DAICHI"), a Japanese satellite, has potentials to observe the marshes under the snow layer. The microwave radar measures the back-scattered signals and works in all weathers. The microwave generally reaches the subsurface layer, so the returned signal includes information about soil moisture as well as surface roughness. We analyze the data from PALSAR and try to retrieve the hydrological information in highland marshes through the year.

Based on our analysis of PALSAR/ALOS data, we lastly reported that the Oze highland marsh, extending across the 4 prefectures (Fukushima, Gumma, Niigata and Tochigi), keeps a largest amount of liquid water body in midwinter, however, no such case seems to happen in Kiritappu and Sarobetsu marshes both locating at Hokkaido. All 3 marshes are covered with snow layer in winter. The peak of water content in Oze is observed in midwinter and not in early spring. We concluded that the observed water body in Oze marsh is not meltwater but would be the liquid water squeezed out from the peat bed by the load of heavy snow. In the other 2 marshes of Kiritappu and Sarobetsu, the thickness of the snow layer and/or peat layer (which is a reservoir of water) seems not enough.

In this presentation, we show our new analysis about Tashiroyama, Uryunuma and Midagahara marshes, locating at Fukushima, Hokkaido and Toyama prefectures, respectively. All 3 marshes are highland marshes where it snows in every winter. We examined whether the water infiltration out of the peat layer could be observed in these highland marshes based on the PALSAR/ALOS data. In both Tashiroyama marsh and Uryunuma marsh, water infiltration was observed during midwinter. In Midagahara marsh, on the other hand, no infiltration of water was observed. We discuss the condition for water infiltration in its correlation with peat depth and snow depth. We propose that water infiltration in highland marshes is caused when the following two conditions are met: 1) layer >2m for the thickness of peat bed and 2) snow cover >2-3m.

Keywords: PALSAR, hydrology, remote sensing, highland marsh, snow, peat bed

An application of ALOS-2 data for study of glacial region

YAMANOKUCHI, Tsutomu^{1*} ; DOI, Koichiro² ; NAKAMURA, Kazuki³ ; AOKI, Shigeru⁴

¹Remote Sensing Technology Center of Japan, ²National Institute for Polar Research, ³Nihon University, ⁴Institute for Low Temperature Science, Hokkaido University

ALOS-2/ PALSAR-2 successfully launched on 24, May, 2014 and it has been collecting the data all over the world properly. The major difference between ALOS and ALOS-2 are improvement of spatial resolution, short revisit cycle, keeping short baseline and improvement of observation opportunity by left-right looking. Among them, the important improvement are short base line and short revisit cycle because it is expected to provide the high coherency between observations. It is able to observe in 14 days difference in the best case, it is almost 3 times shorter temporal difference than ALOS data.

Based on these difference, we choose two area for the comparison between ALOS-2 and ALOS data. One is Mt. El Salto, Andes region. This area has many rock glaciers and we successfully detected the movement of them. Here we would like to check whether ALOS-2 can detect these Phenomenon as ALOS data. The other target area is East Antarctic marginal zone between ice sheet and ice shelf. We already confirmed that the possibility of the extraction of grounding line by PALSAR data and how it improve using ALOS-2 data to take into the effect of short revisit cycle and short baseline. We plan to report how ALOS-2 data be useful for cryospheric study based on these two case studies.

ALOS-2/PALSAR-2 and ALOS/PALSAR data were provided by Research Announcement by JAXA PI project (PI No. P1418002)

Keywords: ALOS-2, SAR, InSAR, grounding line, glacier

An approach to improve the accuracy of ice flow rate measurement of Antarctic ice sheet using DInSAR method

SHIRAMIZU, Kaoru^{1*} ; DOI, Koichiro² ; AOYAMA, Yuichi²

¹SOKENDAI (The Graduate University for Advanced Studies), ²National Institute of Polar Research

Differential Interferometric Synthetic Aperture Radar (DInSAR) is an effective tool to measure the flow rate of slow flowing ice streams on Antarctic ice sheet with high resolution. Since few studies had been made on accuracy estimate of the ice flow measurement using DInSAR method, it is an important subject to discuss the displacements and their changes.

We use Digital Elevation Model (DEM) at two times in the estimating ice flow rate by DInSAR. At first, we use it to remove topographic fringes from InSAR images. And then, it is used to project obtained displacements along Line-Of-Sight (LOS) direction to the actual flow direction. ASTER-GDEM widely-used for InSAR processing of the data of polar region has a lot of errors especially in the inland ice sheet area. Thus the errors yield irregular flow rates and directions. Therefore, quality of DEM has a substantial influence on the ice flow rate measurement.

In this study, we tried to improve estimate accuracy of ice flow rate estimated by DInSAR method by applying a newly created DEM (hereinafter referred to as PRISM-DEM), and compared PRISM-DEM and ASTER-GDEM. Since it is not likely that crustal displacement occurs on outcrops in Antarctica during the recurrence period (in the case of ALOS: 46days), the observed displacements on outcrops are considered to be caused by errors contained in DInSAR images. Therefore, we used the displacements on outcrops as an indicator of error evaluation.

The study area is around Skallen, 90km south from Syowa Station, in the southern part of Soya Coast, East Antarctica. For making DInSAR images, we used ALOS/PALSAR data of 13 pairs (Path633, Row 5710-5720), observed 2007/11/23-2011/1/16. PRISM-DEM covering PALSAR area was created from stereo disparity of nadir and backward images of ALOS/PRISM (Observation date: 2009/1/18, Path187, Row (nadir)5020-5030, (backward)5075-5085).

The number of irregular values of actual ice flow rate was reduced by applying PRISM-DEM compared with that by applying ASTER-GDEM. Additionally, an averaged displacement of approximately 0.74cm was obtained by applying PRISM-DEM over outcrop area, while an averaged displacement of approximately 1.65 cm was observed by applying ASTER-GDEM.

It is concluded that the accuracy of the ice flow rate measurement and errors contained in DInSAR images can be improved by using PRISM-DEM. In this presentation, we will show the results of the estimated flow rate of ice streams, and discuss the accuracy validation of PRISM-DEM.

Keywords: DInSAR, Antarctic Ice Sheet, ice flow rate, DEM

Advanced Land Observing Satellite-2: Mission Status and Forest Observation

SHIMADA, Masanobu^{1*} ; WATANABE, Manabu¹ ; MOTOHKA, Takeshi¹

¹Japan Aerospace Exploration Agency, ²Tokyo Denki University

Advanced Land Observation Satellite-2 (ALOS-2) was launched on May 24, 2014, carrying the L-band Synthetic Aperture Radar (PALSAR-2) to the low polar orbit of 628km-height with 14-day revisit time. To the four mission objectives, i.e., 1) disaster mitigation, 2) environmental monitoring represented by the forest monitoring and cryospheric monitoring, 3) land monitoring, and 4) technology development, PALSAR-2 and ALOS-2 provide the 1~3m high resolution Spotlight and Strip with multi polarization with an imaging swath of 50~70km, ScanSAR imaging with 350~490km swath with dual polarizations, shorter temporal baseline of 14 days and spatial baseline of within 500m of radius, shorter time delay of less than 72 hours (74 hours in worst case) for emergency observation request to the disaster area, and almost all of global beam synchronization for ScanSAR Interferometry. ALOS-2 science program initiates the JAXA's Calibration, Validation, Application researches of the PALSAR-2/ALOS-2 and Pi-SAR-L2. As the application research, the disaster mitigation and the urban area monitoring using the high-resolution data should contribute significantly to the human society since the disasters occur frequently and globally. High resolution and multi polarimetric SAR with the shorter revisit time reserves the quicker detection of the land changes. In this presentation, we will summarize the contents of the ALOS-2 science program, its expected outcomes, and comparative study results with PALSAR.

Keywords: L-band SAR, Forest Observation, Calibration and validation, SAR interferometry

Examination of InSAR tropospheric delay correction with JRA-55 reanalysis data

KINOSHITA, Youhei^{1*} ; FURUYA, Masato¹

¹Department of Natural History Sciences, Hokkaido University

Interferometric Synthetic Aperture Radar (InSAR) phase signal contains not only surface deformations but also propagation delays due to Earth's atmosphere, which is the principal limiting factor for InSAR application of small deformation with amplitude of a few centimeters or less. The atmospheric propagation delay is caused by the difference of refractive index between in atmosphere and in vacuum, and can be divided into the ionospheric delay and the tropospheric delay (Doin et al., 2009). Bevis et al. (1992) showed that the tropospheric delay consists of the hydrostatic delay due to dry gases and the wet delay due to water vapor. In the case of InSAR, the hydrostatic delay can be negligible and therefore the principal source of the tropospheric delay is due to the heterogeneity of water vapor in time and in space (Zebker et al., 1997). Previous studies proposed correction methods which used GNSS delay data or numerical weather model outputs. However, it is still insignificant for detecting small surface deformation.

Jolivet et al. (2014) showed that reanalysis data like ECMWF Interim Re-Analysis (ERA-Interim) data is useful to mitigate topography-correlated tropospheric delay from InSAR data. However, previous studies used only one of the model data as a case study and didn't apply the correction to other areas.

In this study we examined an effect of the tropospheric delay correction with Japanese 55-year reanalysis (JRA-55) data that is designed to produce a high-quality homogeneous climate dataset covering the last half century (Kobayashi et al., 2015). The horizontal resolution of JRA-55 is TL319 (approximately 60 km) and has 60 vertical layers. JRA-55 data are available every six hours. Pressure, temperature and specific humidity are interpolated to the SAR acquisition time and then used to calculate refractive index. We used the calculation method proposed by Jolivet et al. (2014) to estimate the tropospheric delay in the zenith direction and then converted to the line-of sight direction with a simple trigonometric function. In addition, we estimated the tropospheric delay with ERA-Interim data for comparison. SAR data used were derived from ALOS/PALSAR around Nagoya prefecture (Path-Frame: 411-690). We used the GAMMA software to generate interferograms and the 10 m-mesh digital ellipsoidal height model generated by the GeoSpatial Information Authority of Japan to remove the topographic fringe. To avoid the spatial decorrelation, interferometric pairs with the perpendicular baseline of less 3000 m were generated. As a result, 309 interferograms were generated from 28 SAR single-look complex images. Although some of interferograms have long-wavelength phase variations that may be caused by orbital estimation error or ionospheric disturbance, we didn't apply polynomial fitting to remove it because of the difficulty to determine whether that variation are due to the tropospheric delay or not.

In consequence of the tropospheric delay correction with JRA-55 and ERA-Interim data, the averaged standard deviation of all interferograms slightly reduced from 1.26716 cm to 1.25231 cm by JRA-55 and slightly increased to 1.26797 cm by ERA-Interim. We further examined the correction effect when dividing the estimated delay into the hydrostatic component and the wet component. In JRA-55, the averaged standard deviation slightly reduced to 1.26053 cm and 1.2659 cm by applying the hydrostatic and wet delay correction, respectively. On the other hand, in ERA-Interim, the averaged standard deviation slightly reduced to 1.26223 cm and 1.2659 cm by applying the hydrostatic delay correction and increased to 1.28106 cm by applying the wet delay correction. These results indicate that one of the factors of correction failure by ERA-Interim would be due to the low reproducibility of the actual wet delay.

In the presentation, we will report correction effects of JRA-55 and ERA-Interim, and discuss the difference of these effects.

Keywords: InSAR, tropospheric delay, reanalysis data, JRA-55, ERA-Interim

PALSAR-2/InSAR analysis using RINC

OZAWA, Taku^{1*}; MIYAGI, Yosuke¹

¹National Research Institute for Earth Science and Disaster Prevention

Advanced Land Observing Satellite-2 (ALOS-2) was launched on 24 May 2014, and distribution of PALSAR-2 (SAR sensor onboard on ALOS-2) data was began in 25 Nov. 2014. On the other hand, we are developing InSAR tools, named RINC, for researching on advanced SAR analysis techniques using PALSAR-2 and other SAR data (e.g., Ozawa, 2014). In this presentation, we introduce some case studies of PALSAR-2/InSAR analysis using RINC.

PALSAR-2 has three observation modes; stripmap, ScanSAR, and Spotlight. In InSAR analysis using stripmap mode data, high coherence was obtained for most pairs and topographic and orbital phase components could be removed by simulation based on orbit data included in images. Then we applied PALSAR-2/InSAR analysis to the Kuchinoerabujima (volcanic island) and the Ontake volcano and detected phase differences which may be due to surface deformation around the crater. In Ogasawara-Iwoto, obvious crustal deformation associated with volcanic activity was obtained. For the Northern Nagano Earthquake occurred on 22 Nov. 2014, we applied PALSAR-2/InSAR and detected crustal deformation associated with the earthquake.

We attempted to apply InSAR analysis to ScanSAR mode data (490km swath), and obtained fringes in the whole image, although coherence was low. Phase gap among swaths was negligible. However phase difference with long wavelength was remained in the differential interferogram. We attempted to apply InSAR analysis to spotlight mode images for Ogasawara-Iwoto, and high coherence could be obtained. However, artificial phase gap was obtained. These are severe problems on detection of surface deformation, and then its resolution is necessary.

Keywords: PALSAR-2, InSAR, RINC, Kuchinoerabujima, Ontake, the northern Nagano Earthquake

Usefulness of long-term monitoring of volcanic eruptions by synthetic aperture radar

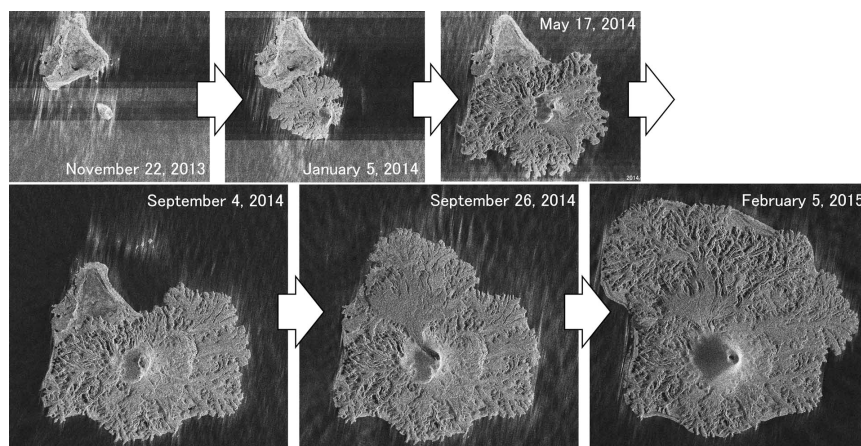
HONDA, Takeshi^{1*} ; UDONO, Toshiaki¹ ; SHIMOMURA, Hiroyuki¹ ; NOZAKI, Takayoshi¹ ; NAKADA, Setsuya² ;
KANEKO, Takayuki² ; MAENO, Fukashi²

¹PASCO CORPORATION, ²Earthquake Research Institute, The University of Tokyo

Nishinoshima is desert island located in about 1000km south from Tokyo. In November 20, 2013, a new eruption was confirmed in the southeast about 500m of the location of Nishinoshima Island, and integrated with the Nishinoshima Island in December 26, 2013, and most of Nishinoshima Island covered by lava in October, 2014. Like these, the active eruption with overflow of lava is also continuing now. However, because Nishinoshima Island is about 130km far from the nearest inhabited islands Ogasawara, it is difficult to observe all the time by eyesight and observation machinery. Although it is possible to monitor from the sky by an aircraft, the aircraft fault is also concerned with the eruption.

The authors, for the purpose of precisely recording the development form of volcanic island, and long term observed using a synthetic aperture radar satellites can be safely and periodically observed.

Keywords: Synthetic aperture radar, Volcano monitoring



©2015 DLR, Distribution Airbus DS / Infoterra GmbH, Sub-Distribution [PASCO]

A spatial filter adaptive to slope size applied to differential SAR interferograms for landslide detection

KUSANO, Shunichi^{1*} ; SANGO, Daisuke¹ ; YAMANOKUCHI, Tsutomu² ; SHIMADA, Masanobu³

¹PASCO corporation, ²Remote Sensing Technology Center of Japan, ³Japan Aerospace Exploration Agency

Differential interferometric SAR (DInSAR) is the technique to measure small surface deformation induced between acquisition times by measuring ground surface several times from satellite. Since it employs microwave, it can observe ground surface of dozens of kilometers square under cloud or volcanic smoke. Thus, DInSAR has been used for the ground subsidence and volcano monitoring.

In the DInSAR image, surface deformation is appeared as an interferometric fringe. On the other hand, the fringe caused by the change of atmospheric water vapor distribution between SAR acquisitions also appears frequently in the image. The fringe caused by the atmospheric effect not only hinders image interpretation but also makes an error in the estimation of surface displacement. In order to make a proper interpretation of local fringes caused by landslide and analyze them quantitatively, it is necessary to remove the fringe caused by the atmospheric effect.

We propose a spatial filter for DInSAR image which suppresses the fringes caused by the atmospheric effect while preserving those caused by landslide as clear as possible. The proposed filter is based on high-pass filter in the spatial frequency domain. The scale of the fringe caused by the atmospheric effect ranges, in general, from several hundred meters to several kilometers, while those caused by landslide is restricted by landslide itself whose size ranges, in general, from dozens meters to several hundred meters in Japan. Using this difference of the scale between the two fringes, one can suppresses the fringes caused by the atmospheric effect efficiently while preserving those caused by landslide.

However, in general, the scale of landslides differs depending on locations. In addition, the shape of landslides is also various and anisotropic. Thus, when detecting a fringe caused by an unknown landslide from DInSAR images, it is difficult to set the appropriate maximal size to be filtered. One needs to adjust the frequency through try and error. To avoid this, the proposed filter is adapted to the size of ground slopes by assuming that the size of landslides is restricted by its underlying ground slope. When filtering, the maximal size is decided based on the size of the slope. Thus, the fringes caused by landslide are preserved adaptively while suppressing those caused by the atmospheric effect.

The procedure of the proposed method is as follows. The slope is defined by the slope orientation angle in this research. In the image of the orientation angle calculated from DEM, pixels with similar values are merged and regarded as the identical slope. The merging is performed by the region growing method. By applying the two-dimensional Fourier transform to the binary image of the detected slope area, the power spectrum is generated. The spectrum is normalized to be a window function and applied to the spectrum generated from DInSAR image of the corresponding area. In this way, the filter is adaptively applied to each slope area. The filtered spectrum of the DInSAR image is transformed to the spatial domain, generating the filtered DInSAR image of the corresponding slope area. By applying the procedure to neighboring slopes, the filter is applied to whole the DInSAR image. In this research, the maximal size of the slope is defined so that the maximal size to be filtered is restricted.

The proposed method was evaluated applying to the DInSAR image of landslide area in Nagano and Yamagata prefecture, Japan. We compared two filters; high-pass filter and proposed filter. By the high-pass filter, the fringes caused by the atmospheric effect are better suppressed, as the maximal spatial frequency to be filtered is high, while the fringes caused by landslide become small and weak. The best spatial frequency is difficult to decide. On the other hand, the proposed method also suppresses the fringes caused by the atmospheric effect while preserving those caused by landslide.

Keywords: Differential SAR interferometry, landslide, spatial filter

Monitoring of Sakurajima Volcano using X-band and L-band SAR

MIYAGI, Yosuke^{1*} ; OZAWA, Taku¹ ; SHIMADA, Masanobu²

¹National Research Institute for Earth Science and Disaster Prevention, ²Japan Aerospace Exploration Agency

Sakurajima volcano is located in southwestern part of Japan, and currently one of the most active volcanoes in Japan. Eruptive activities from a Showa-crater have activated since 2009, and many explosive eruptions have occurred and lava dome growth was found in January 2015. In previous studies, regional and local deformation were detected by GPS, tiltmeter, and leveling [Iguchi et al., 2013; Yamamoto et al., 2013]. To understand current condition and future unrest of Sakurajima, periodic monitoring is required. Although it is generally difficult to make a field observation in dangerous active volcanoes, a satellite remote sensing can make observations of even ongoing volcanoes periodically. Especially, Synthetic Aperture Radar (SAR) sensor is well-suited for monitoring active volcanoes because it can penetrate ash clouds and can observe targets like an active vent. Moreover, SAR data are applicable to use a Differential Interferometric SAR (DInSAR) technique to detect crustal movement associated with the magmatic activities. In this study, we used COSMO-SkyMed (CSK) data through JAXA-ASI co-operative research and ALOS-2/PALSAR-2 data. And we tried DInSAR/PSInSAR processing.

We have been monitoring on Sakurajima volcano using CSK data acquired between 2010 and 2014 from both ascending and descending orbits. From amplitude images, we detected apparent changes of backscattering intensity probably due to an enlargement of the Showa-crater. Because enough coherence could be given by only short-term pairs and the crustal movement on Sakurajima is small, it was hard to detect signals from the DInSAR processing. Then we tried PSInSAR processing using StaMPS software [Hooper et al., 2007]. The results show 1cm/year uplift in north part of Sakurajima volcano between 2012 and 2014, and it corresponds to results from leveling survey. ALOS-2/PALSAR-2 launched in May 2014, and the data have been acquired from both ascending and descending orbits since September 2014. We will introduce the latest result using ALOS-2/PALSAR-2 data.

Keywords: Synthetic Aperture Radar, Sakurajima, Monitoring, InSAR, PSInSAR, Deformation

Spatial distribution of permafrost in the northern Tien Shan, Central Asia

YAMAMURA, Akiko^{1*}; NARAMA, Chiyuki²; TOMIYAMA, Nobuhiro³; TADONO, Takeo⁴

¹Department of Environmental Science, Niigata University, ²Niigata University, Department of Environmental Science, ³Remote Sensing Technology Center of Japan (RESTEC), ⁴Japan Aerospace Exploration Agency (JAXA)

Tien Shan Mountains in the arid and semi-arid regions of Central Asia, with their water resources in the form of mountain glaciers and permafrost, are known as the water towers of Central Asia. Although it is necessary to investigate the current level of these mountain glaciers and permafrost to estimate the amount of water stored (Sorg et al., 2012), the spatial distribution of permafrost is not well known in the northern Tien Shan. We clarify the current state of mountain permafrost in the Kyrgyz Ala-Too Range using the distribution, classification, and motion of rock glaciers as indicators of mountain permafrost.

We applied DInSAR analysis to rock glaciers which identified by field surveys and interpretation of aerial photographs. We extracted the active and inactive rock glaciers according to the motion of rock glaciers. To validate the detected surface motion on rock glaciers, we conducted GPS measurements on rock glacier in Sokuluk Valley. The average movement was 75cm/yr on the glacier-origin rock glaciers between 2013 and 2014. In addition, ground surface temperature shows that the geothermal conditions were sufficient to maintain mountain permafrost inside rock glaciers at the study site.

The distribution of the active and inactive rock glaciers that confirmed their motion revealed discontinuous permafrost altitudinal zones located above 2900 m a.s.l. in the northern part and above 3400 m in the southern part of the Kyrgyz Ala-Too Range. In addition, we confirmed local subsidence between around 3300-3500 m a.s.l. related to the melting of mountain permafrost inside the rock glaciers during summer by short term DInSAR. Half of the active and inactive rock glaciers are glacier-origin type. We also report the environment conditions of glacier-origin rock glaciers.

Keywords: DInSAR analysis, mountain permafrost, rock glacier, Tien Shan

Detection of irregular change of ice sheet in north-western Greenland using ALOS/PALSAR data

DOI, Koichiro^{1*} ; YAMANOKUCHI, Tsutomu³ ; NAKAMURA, Kazuki⁴ ; SHIRAMIZU, Kaoru²

¹National Institute of Polar Research, ²Graduate University for Advanced Studies (SOKENDAI), ³Remote Sensing Technology Center, ⁴Nihon University

Under the situation of ongoing rapid ice sheet melting in Greenland, it is likely that the ice sheet flow velocity is changing there. We applied differential interferometric synthetic aperture radar (DInSAR) to several SAR scenes of north-western Greenland observed by ALOS/PALSAR and the obtained displacement maps had been shown in JpGU2014 as well as maps of the displacement difference obtained by double DInSAR (DDInSAR) technique which means taking the difference between two DInSAR images.

Stable ice flow is a dominant component of surface displacements over ice sheet. Since phase change in a differential SAR interferogram induced by steady surface displacement is canceled out by taking the difference, we can detect irregular surface displacement such as ice sheet flow rate change by DDInSAR.

In order to detect irregular displacement, the DDInSAR technique was applied to an ALOS/PALSAR scene (path-frame: 76-1590) which was observed at three times in series at August 30, October 15, and November 30 in 2007. Two maps of displacement along radar illumination direction have been obtained from the two DInSAR images and a map of displacement difference has been obtained from the DDInSAR image. In the displacement difference map, we found several spots of circular or elliptical shape where displacement differences of 10 to 15 cm were observed. Because the positions of the spots are almost coincident with locations of ponds on the ice sheet near coastal region, these differences seem to be induced by surface displacement of the ponds.

We are going to apply offset tracking technique to the same SAR data to estimate surface flow of the ice sheet and to do further investigation about the displacement differences by combining the surface flow estimated by the technique.

Keywords: Differential Interferometric SAR, ice sheet flow, offset tracking, Greenland

Ground Deformation around the Domestic and Overseas Active Volcanoes detected by ALOS-2/PALSAR-2

ANDO, Shinobu^{1*} ; NAKAHASHI, Masaki² ; ONIZAWA, Shin'ya²

¹MRI, ²JMA

ALOS-2, was launched on May 24, 2014, has an L-band SAR (PALSAR-2) in the same way as ALOS/PALSAR. PALSAR-2 is of help to understand of a ground surface state, and its interferometric coherence is highly effective for the crustal deformation observation. Furthermore, PALSAR-2, is also very short repeat observation cycle (14days), has a higher resolution sensor than PALSAR. Therefore, higher resolution data can be acquired and we analyzed more frequently and are expected to be useful for disaster prevention and mitigation. After the calibration period of about half a year after the launch, ALOS-2 / PALSAR-2 data has been published on November 25, 2014. Operational plan of ALOS-2 / PALSAR-2 have been focused on the accumulation of the base map at least the first year, but when disasters such as earthquake and volcanic activity occur, has been observed according to circumstances.

We have analyze the ground deformation caused by the earthquake and volcanic activity at domestic and overseas using ALOS-2 / PALSAR-2 data. And then, our analysis results are provided to each department of the JMA, and are used to the study of volcanic activity evaluation and seismic analysis results. In this presentation, we mainly report on the analysis results of around active volcano.

Some of PALSAR data were prepared by the Japan Aerospace Exploration Agency (JAXA) via Coordinating Committee for the Prediction of Volcanic Eruption (CCPVE) as part of the project "ALOS-2 Domestic Demonstration on Disaster Management Application" of the Volcano Working Group. Also, we used some of PALSAR-2 data that are shared within PALSAR Interferometry Consortium to Study our Evolving Land surface (PIXEL). PALSAR-2 data belongs to JAXA. We would like to thank Dr. Ozawa (NIED) for the use of his RINC software. In the process of the InSAR, we used Digital Ellipsoidal Height Model (DEHM) based on "the digital elevation map 10m-mesh" provided by GSI, and Generic Mapping Tools (P.Wessel and W.H.F.Smith, 1999) to prepare illustrations.

Keywords: ALOS-2/PALSAR-2, InSAR, Amplitude image, Active volcano